NASA TECHNICAL MEMORANDUM

NASA TM-77810

UNSTEADY AERODYNAMIC CHARACTERIZATION OF A MILITARY AIRCRAFT IN VERTICAL GUSTS

A. Le Bozec and J. L. Cocquerez

(NASA-TM-77810) UNSTEADY AERODYNAMIC CHARACTERIZATION OF A MILITARY AIRCRAFT IN VERTICAL GUSTS (National Aeronautics and Space Administration) 44 p HC A03/MF A01

N85-21110

Unclas

CSCL 01A G3/02 14481

Translation of "Caracterisation aérodynamique instationnaire d'une avion d'armes en rafales verticales," Association Aéronautique et Astronautique de France, 20th Applied Aerodynamics Colloquium, Toulouse, France, Nov. 8-10, 1983. AAAF Paper NT 83-16, pp. 1-47.

NATIONAL AERONAUTICS AND SPACE ADMINISTRATION
WASHINGTON, DC 20546

FEBRUARY 1985

TABLE OF CONTENTS

UNSTEADY AERODYNAMIC CHARACTERIZATION OF A MILITARY AIRCRAFT IN VERTICAL GUSTS

A. Le Bozec AMD-BA[1] and J. Cocquerez IMFL[2]

1 - INTRODUCTION /2*

The study of aircraft behavior in atmospheric turbulence generally covers several areas which are significantly interrelated: unsteady aerodynamics, structure dynamics, flying qualities, and piloting.

The impact of turbulence on the flight of a military aircraft is one of the factors limiting operational use; it is essentially linked to pilot fatigue conditions and to a decrease in platform stability.

For the new generation of aircraft equipped with overall automatic control, a direct and optimum action with respect to the effects of turbulence has been sought since these aircraft were conceived.

This process requires that the unsteady aerodynamic effects resulting from turbulence be recognized and modeled in order to have a tool to predict and improve aircraft behavior.

For this report, the IMFL and the AMD-BA, working closely together, have developed experiments to characterize the unsteady aerodynamics of military aircraft in vertical gusts.

These experiments involved an existing model, well defined elsewhere.

---

*Numbers in the margin indicate pagination in the foreign text.
[1]Research organization, expansion unknown.
[2]Research organization, expansion unknown.

Following a brief review of the experimental method developed to establish a data base, we present the methods of analysis and aerodynamic characterization used, as well as the principal results obtained.

2 - PRINCIPLES AND EXPERIMENTAL METHOD /3

2.1 - Basic principles - physical similarity

The experiments on a free model are based on the Froude similarity (maintaining the ratio of inertia forces to gravity forces) which allows a similar representation of the trajectory and movement of the aircraft. The variables of the problem are expressed as a function of these primary independent values: gauge length, volumetric mass of the environment, and gravitational acceleration. The principal physical values, their "size," and object-model similarity ratios are presented in Figure 2.

This similarity is limited since, from an aerodynamic point of view, it cannot simultaneously represent the identities of the Reynolds and Mach numbers. We note also that tests on free models relate only to the area of incompressible subsonic flight. In addition, the use of large models makes it possible to reach Reynolds numbers, calculated on the average chord of the blade, in the neighborhood of 2.3×10^6.

The concept of gust response tests is established using an indirect similarity process. The tests on a model constitute experimental support for validating a mathematical model which represents the phenomena. The conditions for the model and for free flights are adapted on a trial-and-error basis.

2.2 - Model and instrumentation /4

Figure 3 presents a general view of the model used in this work. It is a permeable model of the Mirage 2000 scaled at 1/8.6. The internal and external elevons are interdependent. The nose-tip is kept at 0° during all the experiments. The basic centering is 52%.

The model is instrumented to allow, by means of PCM telemetry, recovery of motion dynamics, recovery of positions and attitudes, and determination of aerodynamic values: local kinetic pressure, incidence, and sideslip via an anemoclinometric probe placed on the furthest forward point and used to measure the gust.

The model's equipment includes (Figure 4):

- 5 accelerometers $\ddot{Z}$ AV, $\ddot{Z}$ AR, $\ddot{Y}$ AV, $\ddot{Y}$ AR, $\ddot{X}$
- 1 lateral gyrometer p
- 1 anemoclinometric probe linked to 3 pressure transducers (local kinetic pressure, incidence, sideslip)
- 1 coder-transmitter unit, PCM mode, 30 measuring tracks
- 1 cell for acquisition initialization and space-time synchronization
- 1 scanner for measuring the initial drop velocity
- 3 reference points for trajectory calculation
- internal powerpacks.

The accelerometers used are limited accelerometers with a frequency in excess of 800 Hz.

The gyrometer acts as a second level, with cut-off frequency of 45 Hz and absorption coefficient of 0.8.

The pressure transducers have their own frequency of 5000 Hz. The low-pass filters are interposed before coding and emission. The longitudinal parameters ($\ddot{Z}$ AV, $\ddot{Z}$ AR, α probe) are low-pass filtered, cut-off frequency 150 Hz, fourth level with the goal of avoiding scale-folding problems caused by the sampling. The signals from the transducers are coded in PCM mode at 12 bits, the frequency of the coder is 150 kbits/second, and 30 measuring tracks are available. Each parameter appears twice in the cycle, which corresponds to a sampling period of 1.28 ms (781 Hz). /5

2.3 - Vertical gust generator (Figure 5)

The vertical gust generator occupies at maximum the volume left free by the lateral wind tunnel. It generates a stream semi-guided by the two lateral return corridors; the working section of the stream, located 2 m above ground, is 2.75 m high, 3.30 m wide, and 2.5 m long. It is inclined 4° from the vertical to minimize the X component.

Three longitudinally distributed profiles of vertical velocity were created for these tests (Figure 6): one of window type, one of rising gradient type, and one of descending gradient type. These three types of profiles allow us to test the influence that frequency distribution at the entrance has on model response. The maximum velocity for each profile is 2.5 m/s, which makes it possible to obtain a variation of incidence compatible with the hypotheses of linearity of the model, while allowing for the model velocity (35 m/s). These profiles were formed through the use of flow distribution grates placed in the blowing and suction chambers.

The profiles of gust types are identified by three series /6
of velocity measurements taken with a micro-windmill in three parallel planes, situated on the flight symmetry axis and 0.25 m

to either side of the axis, at a height corresponding to the average passing altitude of the model in the wind tunnel. The repeatability and the stability of the gust over time have been verified, which guarantees that the gust crossed during the test conforms to the gust previously measured.

2.4 - Catapulted flight test station

In the general view of the testing installation (Figure 7), it is possible to distinguish the zone where wind velocity is increased and decreased using a pneumatic catapult, the free flight area where trajectories can be developed over the approximately 30 m of distance covered, and the model recovery zone. In the free flight area, the vertical gust generator makes it possible to create exterior stresses (incidence) on a length of 2.5 m.

The methods chosen for catapulting the model make it possible to obtain precise initial drop conditions, especially with respect to geometry, kinetics, dynamics (vibratory and instrumental aspects) and aerodynamics.

The initial longitudinal velocity at the time of drop is clearly defined using scanning barriers.

The data necessary for determining the trajectory and attitudes of the model in flight are obtained on three ground bases equipped with banks of scanners. Each base is situated in a vertical plane normal to the flight symmetry plane and includes two optical recording banks with photographic plates at perpendicular axes. Each base thus records the luminous reference trails made by the model, as well as a fixed local reference. The trails are picked up continuously. Pre-programmed triggered flashes make a freeze-frame of the model on /7

each photographic plate and activate a photocell on the model. This photocell generates space-time synchronization data inserted in the PCM telemetry cycle.

2.5 - Software for interpreting test results (Figure 8)

Two principal programs are used to process free flight data:

- a trajectory calculation program processes the luminous spatial reference trails made by the model, using data obtained by processing scanner recordings from the bases. From this are obtained the Euler angles, the center of gravity coordinates, and the velocity vector orientation for each base.

- a program for processing the telemetry data uses the values obtained from the difference between free flight and zero readings made under the catapult immediately before velocity is increased. The first unit of initial conditions is determined either by direct measurements (instantaneous values furnished by the transducers at the time of velocity drop) or by independent measurements (slope, attitudes, initial velocity, etc.).

The results obtained from these two independent sources of information are then used in a test for validating data and for final adjustment of the initial flight conditions. Trajectory calculation data remain the most precise and make it possible to establish points of coincidence with the integrated dynamic data. Flights are valid when, for each variable, the coincidence occurs inside the "precision tubes" defined by the geometric values. Adjustments are made to the initial conditions of the flight (ψ, θ, ϕ, X, Y, Z, first and second derivatives), taking into account the confidence interval of each parameter. /8

Elsewhere, the IMFL is pursuing the development of another recovery method based on Kalman filtering.

3 - METHODS OF RESULT ANALYSIS AND AERODYNAMIC CHARACTERIZATION /9

3.1 - Research of impulse responses (AMD-BA)

Stationary coefficients, it appears, are absolutely not adaptable to modeling an aircraft penetrating a gust (Figure 9).

The moment of pitch is even opposite in sign to that which occurs in reality.

The standard methods of unsteady representation, developed especially at IMFL and based on dividing the aircraft into forward fuselage, wing, and tail section, give good results for civil aircraft but seemed to us to be poorly adapted for a delta wing.

This is why Avions Marcel Dassault has continued to use research on impulse responses as a method of aerodynamic characterization for a military aircraft penetrating a gust.

Once the impulse responses are defined, any type of gust can be considered the sum of impulses. If the aerodynamic phenomena are linear, the aircraft response to any type of gust will be the sum of the impulse responses, the integrals of which are the indicative responses.

The hypothesis of linearity is justified by the range of /10
low incidences in practice.

The aircraft behavior can be characterized by a transfer function H (p) - (Figure 10).

p: Laplace variable

t: time variable

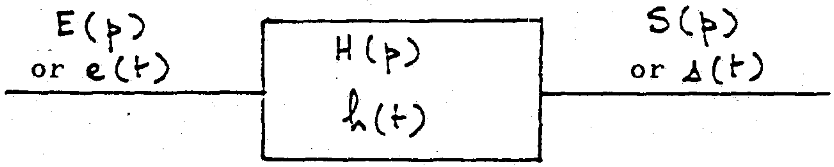

<u>input</u> = gust <u>output</u> = aircraft response

Remember that the functions F(p) and $f(t)$ are relinked in the equation by the Laplace transformation.

$$F(p) = \int_0^{+\infty} f(t)\, e^{-pt}\, dt$$

On the other hand, it is possible to write:

$$S(p) = H(p) \,.\, E(p)$$

or

$$s(t) = h(t) * e(t)$$

*designates a convolution product.

In the case of vertical gusts, as the observed transversal moments in the tests are slight:

- sideslip $\beta \leq 1°$
- lateral attitude $\phi \leq 5°$

only the longitudinal components Cm and Cz are of interest.

Thus it can be written: /11

$$C_z(t) = C_{z_0} + C_{z_q} \cdot q(t) + C_{z_\alpha}(t) * \alpha(t)$$
$$C_m(t) = C_{m_0} + C_{m_q} \cdot q(t) + C_{m_\alpha}(t) * \alpha(t)$$

coefficients measured at time t	unknown constant coef.	dynamic coef. linked to unknown pitch velocity	unknown unsteady coef.	incidence measured at time t

Some authors propose the following representation:

$$C_z(t) = C_{z_0} + C_{z_q} * q(t) + C_{z_\alpha}(t) * \alpha(t)$$
$$C_m(t) = C_{m_0} + C_{m_q} * q(t) + C_{m_\alpha}(t) * \alpha(t)$$

We have not used this representation in the present case, because pitching velocity changes little in the gust.

To explain the convolution product, the following is used:

$$C_{\substack{z\\m}}(t) = C_{\substack{z\\m}0} + C_{\substack{z\\m}q} \cdot q(t) + \int_0^{+\infty} C_{\substack{z\\m}\alpha}(T) \cdot \alpha(t-T)\,dT$$

and to refine it:

$$C_{\substack{z\\m}}(t) = C_{\substack{z\\m}0} + C_{\substack{z\\m}q} \cdot q(t) + \sum_{i=0}^{p} C_{\substack{z\\m}\alpha_i} \cdot \alpha(t-iT)$$

This leads ultimately to resolution of the matrix equation:

$$AX = B$$

matrix of measured "angles of incidence"	matrix of unknown coefficients	matrix of measured coefficients
A (n,p + 3)	X (p + 3, 2)	B (n,2)

3.2 - IMFL Method of "local" coefficient identification /12

To study C.A.G. [expansion unknown] linked to free model tests involving crossings of short wave-length vertical gusts, the IMFL has systematically developed and is developing mathematical models for representing phenomena based on dividing the model into several sections. This method makes it possible to allow for the distribution of aerodynamic incidence on the aircraft.

For a model subjected to a gust of short length with respect to the length of the model, the profile of the vertical velocities is not uniform along the model. This statement leads to the consideration not of one single incidence, calculated at the model's center of gravity, but of a family of local incidences which makes it possible to allow for and to represent the rapidly variable aspect of the phenomenon. These local incidences are calculated at the geometric centers of the various sections (Figure 11).

3.2.1 - Model choice and equations

The hypotheses used for the remainder of the calculation are the following:

- the model is an unchangeable solid;
- the movement of the model is longitudinal;
- the gust is contained in the XOZ vertical plane, the symmetric plane of the model;
- the velocity of the model is constant in the module;
- all angles are considered small; /13
- the gust is permanent (stable during the time the model takes to cross the gust).

Longitudinal movement is described by the equations for lift and moment of pitch.

Projection on Gza

$$-mV(\dot{\alpha} - q) = -\frac{1}{2}\rho S V^2 C_z + mg$$

moment around the center of gravity

$$B\frac{dq}{dt} = \frac{1}{2}\rho S l V^2 C_m$$

STANDARD TITLE PAGE

1. Report No.	2. Government Accession No.	3. Recipient's Catalog No.
NASA TM-77810		

4. Title and Subtitle	5. Report Date
UNSTEADY AERODYNAMIC CHARACTERIZATION OF A MILITARY AIRCRAFT IN VERTICAL GUSTS	February 1985
	6. Performing Organization Code
7. Author(s) A. Le Bozec and J. L. Cocquerez	8. Performing Organization Report No.
	10. Work Unit No.
9. Performing Organization Name and Address The Corporate Word, Inc. 1102 Arrott Bldg. Pittsburgh, PA 15222	11. Contract or Grant No. NASW-4006
	13. Type of Report and Period Covered Translation
12. Sponsoring Agency Name and Address National Aeronautics and Space Administration Washington, DC 20546	14. Sponsoring Agency Code

15. Supplementary Notes Translation of "Caracterisation aerodynamique instationnaire d'une avion d'armes en rafales verticales," Association Aeronautique et Astronautique de France, 20th Applied Aerodynamics Colloquium, Toulouse, France, Nov. 8-10, 1983 (A84-32484). AAAF Paper NT 83-16, pp. 1-47. (A84-32484)

16. Abstract The effects of 2.5 m/sec vertical gusts on the flight characteristics of a 1:8.6 scale model of a Mirage 2000 aircraft in free flight at 35 m/sec over a distance of 30 m are investigated. The wind tunnel setup and instrumentation are described; the impulse-response and local-coefficient-identification analysis methods applied are discussed in detail; and the modification and calibration of the gust-detection probes are reviewed. The results are presented in graphs, and good general agreement is obtained between model calculations using the two analysis methods and the experimental measurements.

17. Key Words (Selected by Author(s))	18. Distribution Statement
	Unlimited

19. Security Classif. (of this report)	20. Security Classif. (of this page)	21. No. of Pages	22. Price
Unclassified	Unclassified	44	

NASA-HQ

The coefficients Cz and Cm are linearized with respect to incidence

$$C_{\underset{m}{z}}(t) = C_{\underset{m}{z}o} + \sum_i C_{\underset{m}{z}\alpha_i} \cdot \alpha_i(t)$$

summation extended to all control points where local incidences are calculated.

$$\alpha_i(t) = \left(\alpha_{CDG} + \frac{w_i}{V} - q\frac{l_i}{V}\right)(t)$$

with α_{CDG} incidence with the ground calculated at the CDG

$\frac{w_i}{V}$ variation of the incidence introduced by the vertical gust, calculated at point i by applying a pure delay to the value measured by the anemoclinometric probe.

$q\frac{l_i}{V}$ influence of the pitching velocity

The local coefficients $Cz_{\alpha i}$ and $Cm_{\alpha i}$ are a result of minimizing an object model distance criterion by least squares: /14

$$J = \sum_t \left[C_{\underset{m}{z}}(t) - \left(C_{\underset{m}{z}o} + \sum_i C_{\underset{m}{z}\alpha_i} \cdot \alpha_i(t)\right)\right]^2$$

The coefficients thus identified are then introduced into the simulation.

3.2.2 – Simulation model

Using the formulated hypotheses, the longitudinal movement equations are written:

$$mV\frac{dV}{dt} = \frac{1}{2}\rho S V^2\left[-\left(\sum_i C_{z\alpha_i}\frac{l_i}{V}\right)q + C_{z\alpha}.\alpha + C_{z_0} + \sum_i C_{z\alpha_i}\frac{w_i}{V}\right] - mg$$

$$B\frac{dq}{dt} = \frac{1}{2}\rho S l V^2\left[-\left(\sum_i C_{m\alpha_i}\frac{l_i}{V}\right)q + C_{m\alpha}.\alpha + C_{m_0} + \sum_i C_{m\alpha_i}\frac{w_i}{V}\right]$$

$$q = \frac{d\gamma}{dt} + \frac{d\alpha}{dt}$$

The matrix form of the differential system is thus written:

$$\dot{x}(t) = \| A \| \cdot x(t) + \| U(t) \|$$

with: $x = \begin{pmatrix} q \\ \alpha \end{pmatrix}$

$$\| A \| = \begin{pmatrix} -\frac{1}{2} \rho \frac{S l V}{B} \sum_i C_{m_{\alpha_i}} l_i & \frac{1}{2} \rho \frac{S l V^2}{B} C_{m_\alpha} \\ \frac{1}{2} \rho \frac{S}{m} \sum_i C_{z_{\alpha_i}} l_i + 1 & -\frac{1}{2} \rho \frac{S V}{m} C_{z_\alpha} \end{pmatrix}$$

$$\| U(t) \| = \begin{pmatrix} \frac{1}{2} \rho \frac{S l V^2}{B} \left(C_{m_0} + \sum_i C_{m_{\alpha_i}} \frac{w_i}{V} \right) \\ -\frac{1}{2} \rho \frac{S V}{m} \left(C_{z_0} + \sum_i C_{z_{\alpha_i}} \frac{w_i}{V} \right) + \frac{g}{V} \end{pmatrix}$$

3.3 - Choice of analysis parameters /15

This essentially concerns incidence. Three values are available:

α_{ground} = ground incidence: This is the angle made by the aircraft velocity vector and the horizontal fuselage reference. These angles are of no interest for the unsteady aspect.

$\alpha_{P} = \alpha_{ground} + \frac{w}{V}$: pressure measurement incidence

where w: gust velocity derived from pressure measurement.

and V: aircraft velocity

probe: incidence measured by the probe

The intensity of the gust, expressed as ΔCz and ΔCm, varies with regard to pressure measurement incidence between tests conducted with the same gust. These differences are clearly more than measurement error.

On the other hand, a clear correlation is observed between the Cz and Cm effects of the gust and the probe incidence. This implies use of the latter for calculating impulse responses (Figure 12).

4 - VERIFICATION OF GUST DETECTION PROBES /16

4.1 - Behavior outside the gust

The first tests made with a spherical probe revealed a noise problem affecting incidence measurement. Analysis showed:

- that it was not a handling problem, as the noise also appeared on the electric signal.

- that it was white noise.

- that it was not electrical in origin. While the transducers are being set at zero, before increasing velocity, the signal does have the noise.

- that the increase of fluctuations with velocity during the acceleration phase on the launch ramp resembles aerodynamic noise (Figure 13).

Explaining the crest-crest incidence deviations of 1.5° requires velocity variations of 0.9 m/s; these are incompatible with "at rest" air conditions in a turbulence-free laboratory.

The conclusion is thus reached that the constant noise is definitely linked to the geometry of the probe.

A series of tests conducted at the CEAT S4 wind tunnel confirmed our conclusions and led us to adopt a probe with conical geometry (Gruson probe), the desired gain being approximately 2 (Figure 14).

Upon retesting in free flight, our expectations were surpassed. The fluctuations were brought to $\Delta\alpha \simeq 0.3°$ crest-crest. /17

4.2 - Behavior in the gust

Tests for measuring probe response time were conducted at Chalais, Meudon. This dynamic standardization, which constitutes the identification of the internal dynamic response of the probe (entire unit - piping - transducer case - transducer), has no bearing on establishing the flow on the probe. For the Gruson probe, the delay taken into account for velocity and incidence signals is 3 ms (1 ms pure delay and 2 ms to climb to 10%).

In the unit, the comparison of probe incidence and pressure measurement incidences is quite good on window gusts, with, however, small deviations on the plateau value (0.4° max.). On the ramps, more significant deviations on the maximum values are noted (Figure 15). However, past records show that probe velocity increases about 1 m/s as the gust passes.

To solve these problems, work was done to characterize the overall dynamic behavior of the probes (aerodynamic aspect).

5 - PRESENTATION OF PRINCIPAL RESULTS /18

5.1 - Steady aspect

5.1.1 - Correlation with wind tunnel results

A catapulted flight with a gust includes four stages:

- one phase to lessen the transitory effects of the ramp (of no interest for this study);

- one phase of passage through the gust;

- two phases of quasi-permanent flight: one before and one after the gust (Figure 16).

The interest in these two last phases concerns the degree of credibility of the measurements made, in comparison to results obtained in other wind tunnels.

It can be confirmed (Figure 17) that values are similiar for:

- the lift gradient
- the polar curve opening
- the position of the center

The Fauga results, which stand out, are perfectly explained by the influence of the Reynolds number.

The wind tunnel curves are reset based upon the null lift values (C_{x0}, δ_{m0}, α_0) of the free flight. These parameters are a function of the mounting and especially the permeability of the model.

5.1.2 - Repeatability /19

Another credibility criterion for the measurements made concerns the repeatability of results; as every experimenter knows, two experiments reputed to be identical do not always give the same results.

From this point of view, the following can be considered satisfied:

$$\Delta\alpha \simeq \pm 0.15^{\circ}$$

$\Delta\delta_m$ balance $\simeq \pm 0.1^{\circ}$

$$100\,\Delta C_x \simeq 0.2$$

(Figure 18)

These values were obtained by constantly improving test procedures, as well as by more specific concentration on elevon rigidity and precision of aileron display; this last parameter is very noticeable for an aircraft with delta wings.

5.2 - Unsteady aspect

5.2.1 - Impulse method (AMD-BA)

The unsteady results are themselves encouraging, as the indicative responses converge well on the steady gradients in most cases (Figure 19).

However, there is still some noise, and identification in the case of some flights gives unsatisfactory results:

- significant oscillations (Figure 20)
- non-convergence

An investigation of these problems is under way, in /20
particular with respect to the impact of structural noises, behavior of gust detection (probe), etc.

5.2.2 - Sectional method (IMFL)

The results presented in Figures 21 and 22, comparing the Cz and Cm obtained in flight to those obtained in simulation with an

overall model (one section) or a model in sections, require the following remarks:

- the overall model, as predicted, does not follow real behavior, especially in pitching response;
- with a model cut into 14 sections, behavior in pitching-pumping is very well restored.

During its development, this method was the subject of additional studies which make it possible to identify especially: the effect of the number of sections, the eventual physical significance of the coefficients, and the durability of the model with regard to various gust entrances.

6 - GENERAL DISCUSSION OF RESULTS AND DEVELOPMENT PERSPECTIVES /21

The experimental method is proven to be well adapted for unsteady aerodynamic characterization in vertical gusts.

The need for the launched probe to take gust intensity into account in the various analysis methods indicates that more complete verification is necessary, especially in dynamics.

The balanced characteristics are heightened beginning with flights outside of gusts, which constitutes a given reference with respect to wind tunnel results.

From an unsteady point of view, the first results are satisfactory. The development perspectives presented for analysis methods and aerodynamic characterization are encouraging and give rise to the necessary investigations.

On the bases presently established, it is possible to simulate an aircraft's behavior in turbulence given its design. This makes it possible to envision treatment of problems concerning behavior optimization through the concept of generalized automatic control.

REFERENCES

Cocquerez, J. L. "Caractérisation expérimentale de la réponse à des rafales d'un avion d'armes avec et sans plans canard [Experimental Characterization of Responses to Gusts of a Military Aircraft With and Without Noseplanes]." IMFL, December 1982.

Cocquerez, J. L. "Etudes de mécanique du vol par maquettes catapultées en laboratoire [Studies of Flight Mechanics by Models Catapulted in a Laboratory]." Association Aeronautique et Astronautique de France, 16th Colloquium, Lille, November 1979.

Coton, P. "Application du filtrage de Kalman à la restitution des trajectoires et des attitudes de maquettes d'avions catapultées en vol libre en laboratoire [Application of Kalman Filtering to the Restoration of Trajectories and Attitudes of Aircraft Models Catapulted into Free Flight in the Laboratory]." IMFL, June 1981.

Coton, P. "Validation de modèles de représentation du comportement des aérodynes en rafales verticales [Validation of Models Representing Aerodyne Behavior in Vertical Gusts]." IMFL, September 1982.

Verbrugge, R. A. and Charon, W. "Nouvelle technique d'essais sur maquettes libres pour la détermination de caractéristiques aérodynamiques [New Free Model Test Techniques for the Determination of Aerodynamic Characteristics]." AGARD C.P. 235, May 1978.

Verbrugge, R. A., Charon, W. and Marchand, M. "Wind Tunnel and Free Flight Model Identification Experiment." AGARD LS 104, 1979.

Figure 1

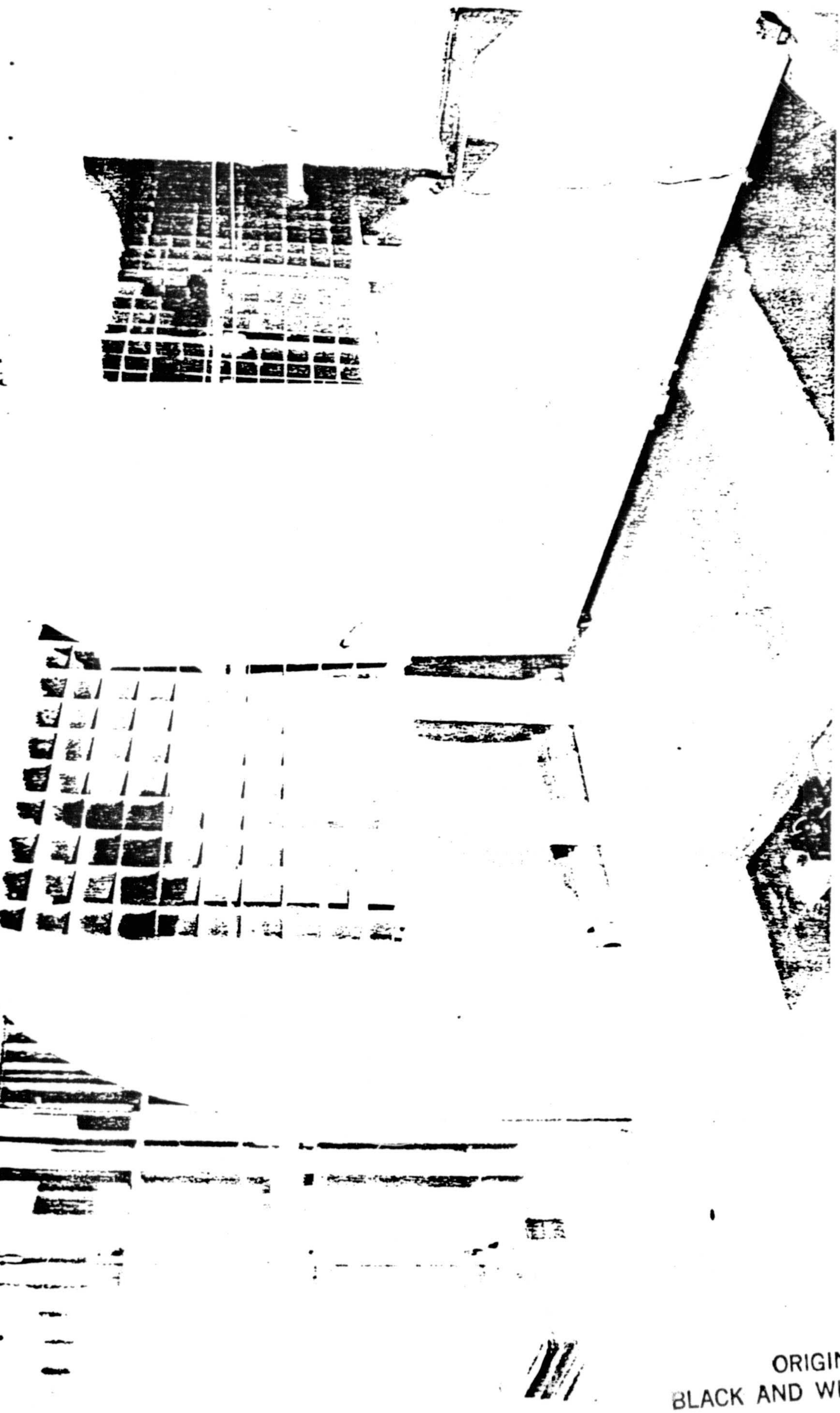

ORIGINAL PAGE
BLACK AND WHITE PHOTOGRAPH

PHYSICAL SIMILARITY

GEOMETRIC SCALE OF MODEL, MODEL BLADE/AIRCRAFT BLADE

RATIO OF VOLUMIC AIRMASSES, ZERO ALTITUDE OF MODEL FLIGHT, ALTITUDE OF AIRCRAFT FLIGHT

VARIABLE	DIMENSION	RELATIONSHIP
LENGTH	L	λ
MASS	M	$m\lambda^3$
TIME	T	$\lambda^{0,5}$
SURFACE	L^2	λ^2
VOLUME	L^3	λ^3
VELOCITY	LT^{-1}	$\lambda^{0,5}$
ACCELERATION	LT^{-2}	1
FREQUENCY	T^{-1}	$\lambda^{-0,5}$
INERTIA	ML^2	$m\lambda^5$
FORCE	MLT^{-2}	$m\lambda^3$
MOMENT	ML^2T^{-2}	$m\lambda^4$
PRESSURE	$ML^{-1}T^{-2}$	$m\lambda$

Figure 3

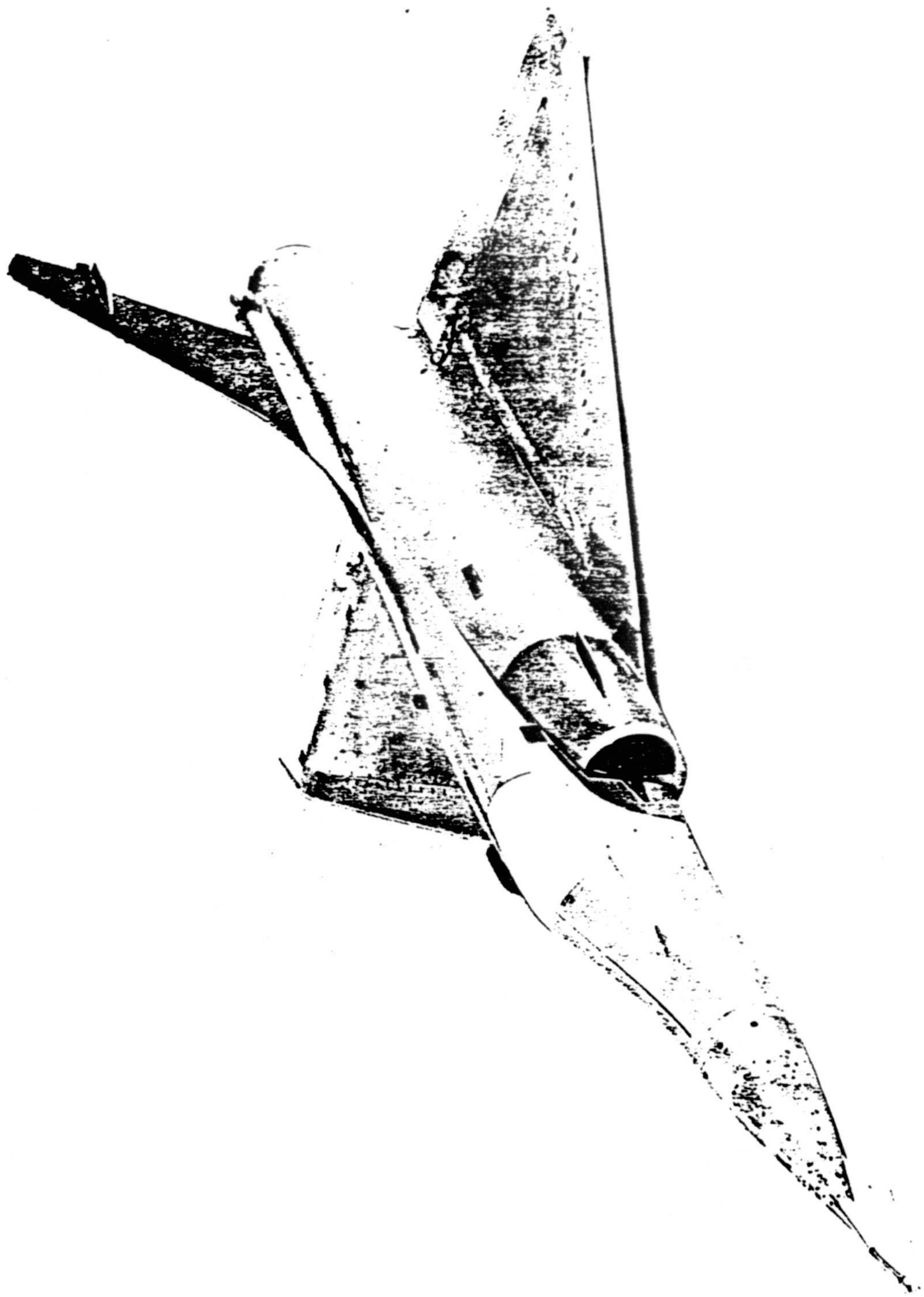

EXPERIMENTAL MODEL

MODEL CHARACTERISTICS AND EQUIPMENT

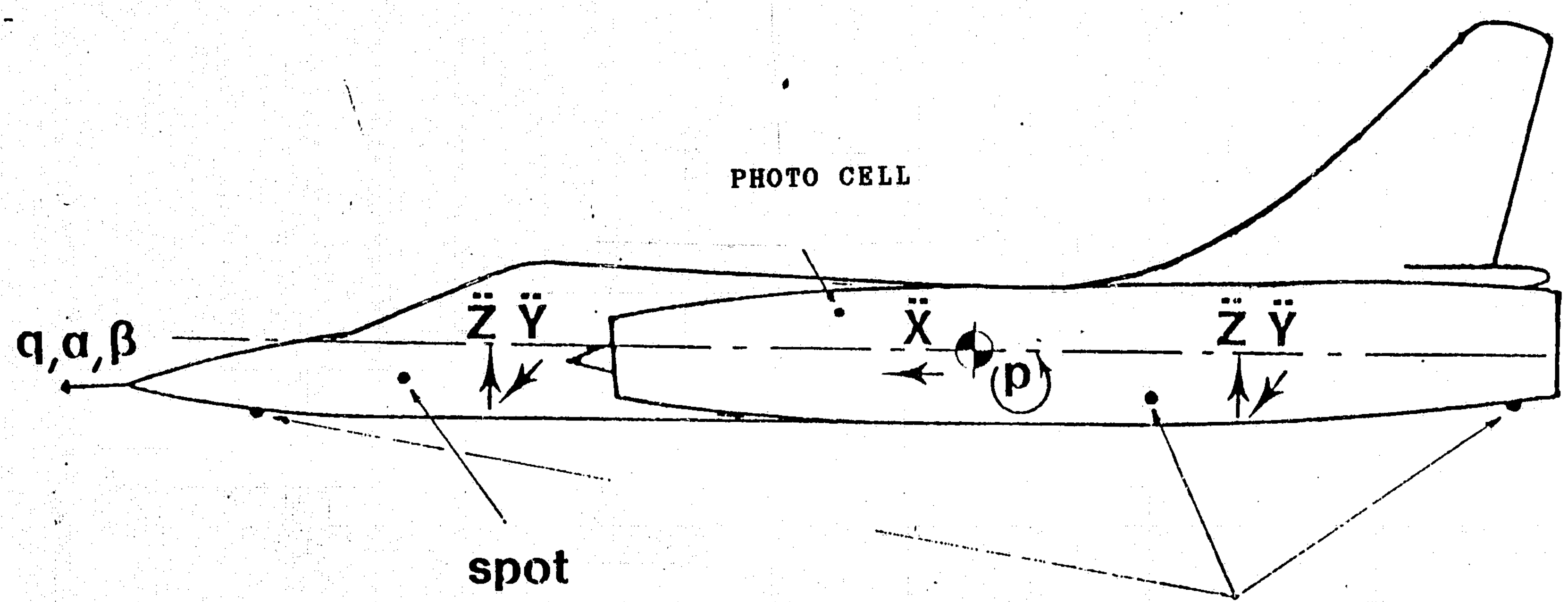

SCALE	1/8.6	MASS	20.3 kg
BLADE	0.965 m	A	0.43 m2.kg
SURFACE	0.554 m2	B	2.50 m2.kg
		C	2.75 m2.kg

ORIGINAL PAGE
... AND WHITE PHOTOGRAPH

Figure 4

VERTICAL GUST GENERATOR

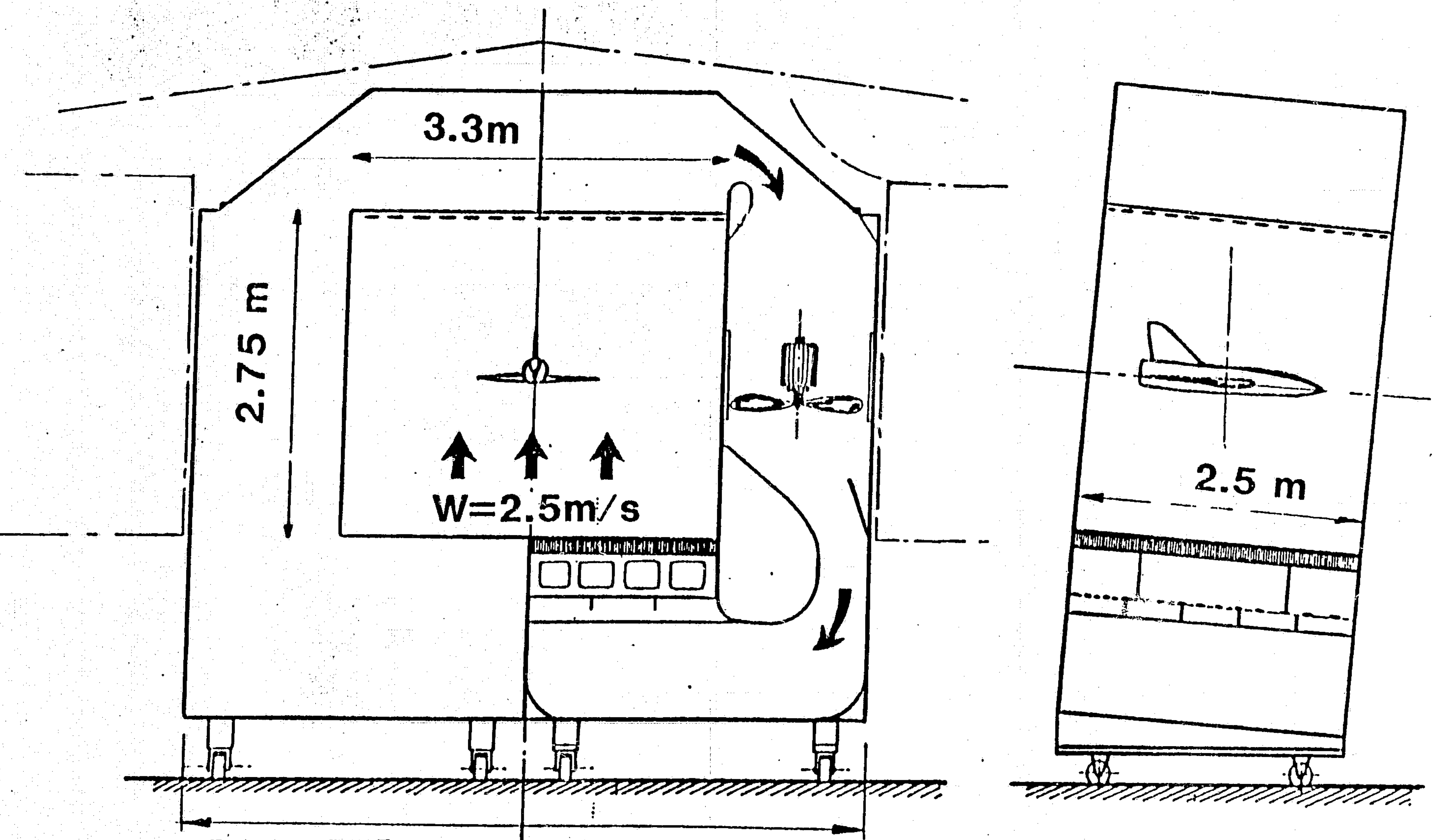

ORIGINAL PAGE
BLACK AND WHITE PHOTOGRAPH

Figure 5

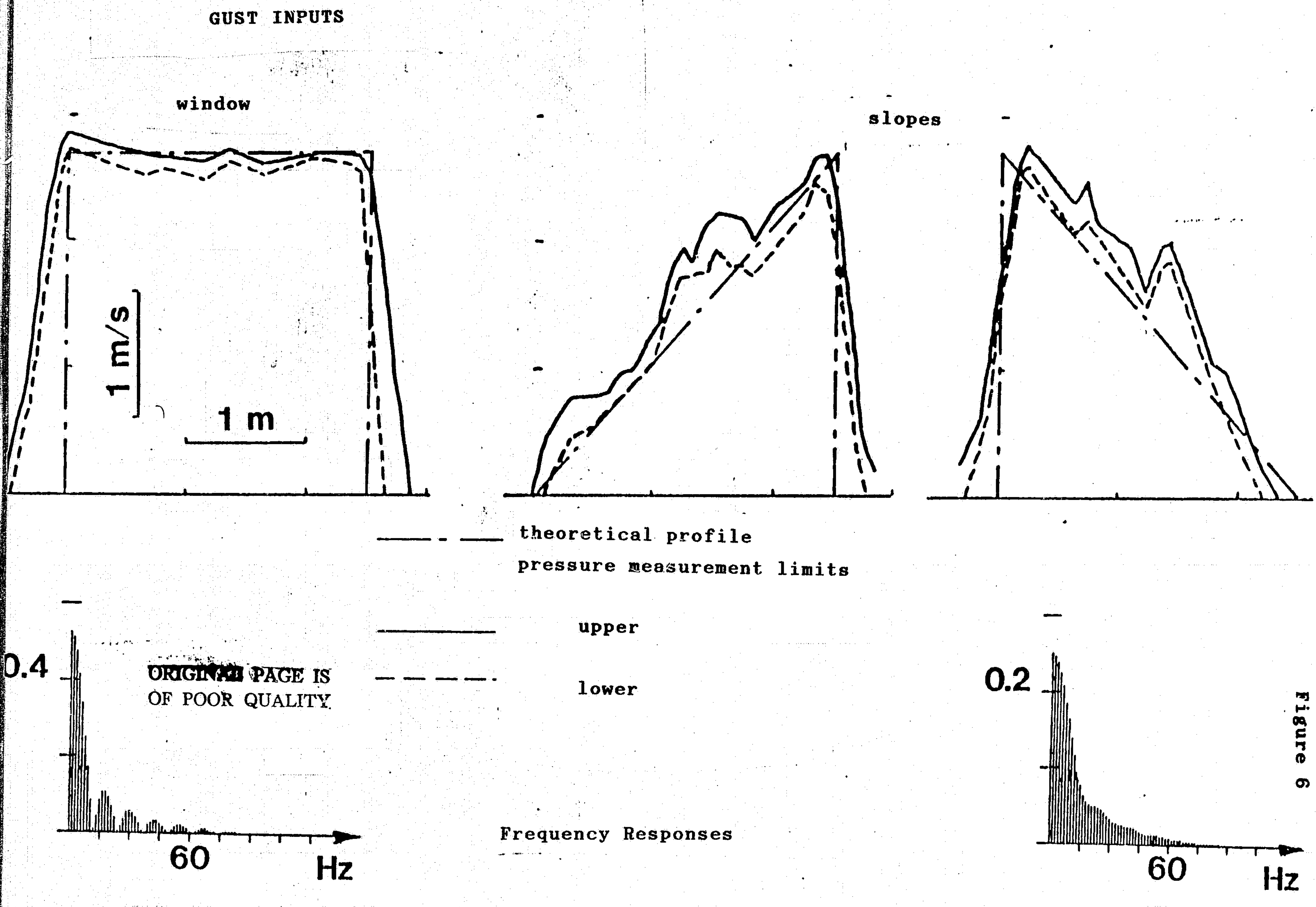

GUST INPUTS
window
slopes
1 m/s
1 m
theoretical profile
pressure measurement limits
upper
lower
0.4
60
Hz
0.2
60
Hz
Frequency Responses

Figure 6

Figure 7

GEOMETRY OF FLIGHT SPACE

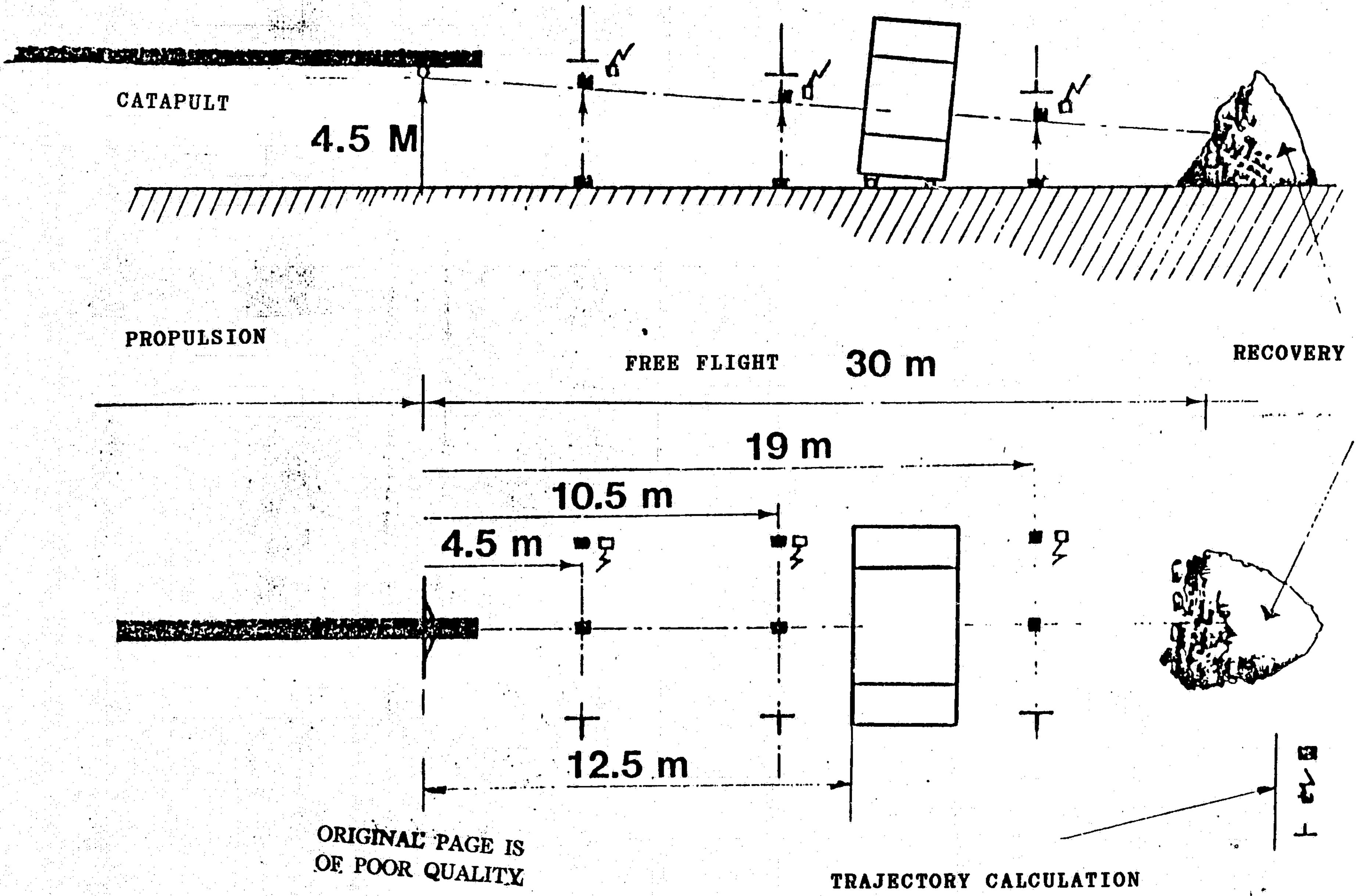

Figure 8

GROUND MEASUREMENTS

OPTICAL TRAJECTORY CALCULATION

<u>DATA</u> SPATIAL REFERENCE TRAILS
MODEL FOR SEVERAL
RECORDING BASES
SCALES AND GEOMETRIC
DEFINITION

MODEL MEASUREMENTS

PCM DYNAMIC RECORDINGS

<u>DATA</u> ACCELEROMETRY,
GYROMETRY, ANEMO-
CLINOMETRY, GOVER-
NING POSITIONS,
SPACE-TIME SYNCHRO
TOPS

<u>RESULTS</u> AT THE MOMENT OF MEASUREMENT,
FOR EACH BASE, VALUE OF EULER'S
ANGLES, OF CDG COORDINATES, AND
OF THE SPATIAL SLOPE'S DIRECTING
COSINES

INITIAL
VELOCITY
AND
CONDITIONS
AT
PITCHING

TREATMENT - VALIDATION TEST

(COMPARISON GROUND MEASUREMENTS/CALCULATIONS FOR
EACH BASE, ELABORATION OF CORRECTIVE TERMS FOR
INTIAL CONDITIONS, ACCORDING TO THE MEASUREMENT
PRECISION CRITERIA)

<u>RESULTS</u> FOR EACH MOMENT OF SAMPLING, EULER'S
ANGLES, CDG COORDINATES AND THE FIRST AND
SECOND DERIVATIVES OF VELOCITY, INCIDENCE,
SIDESLIP, GOVERNING AILERON MOVEMENTS

ELABORATION OF STATUS VARIABLES AND AERODYNAMIC CHARACTERISTICS

Figure 9

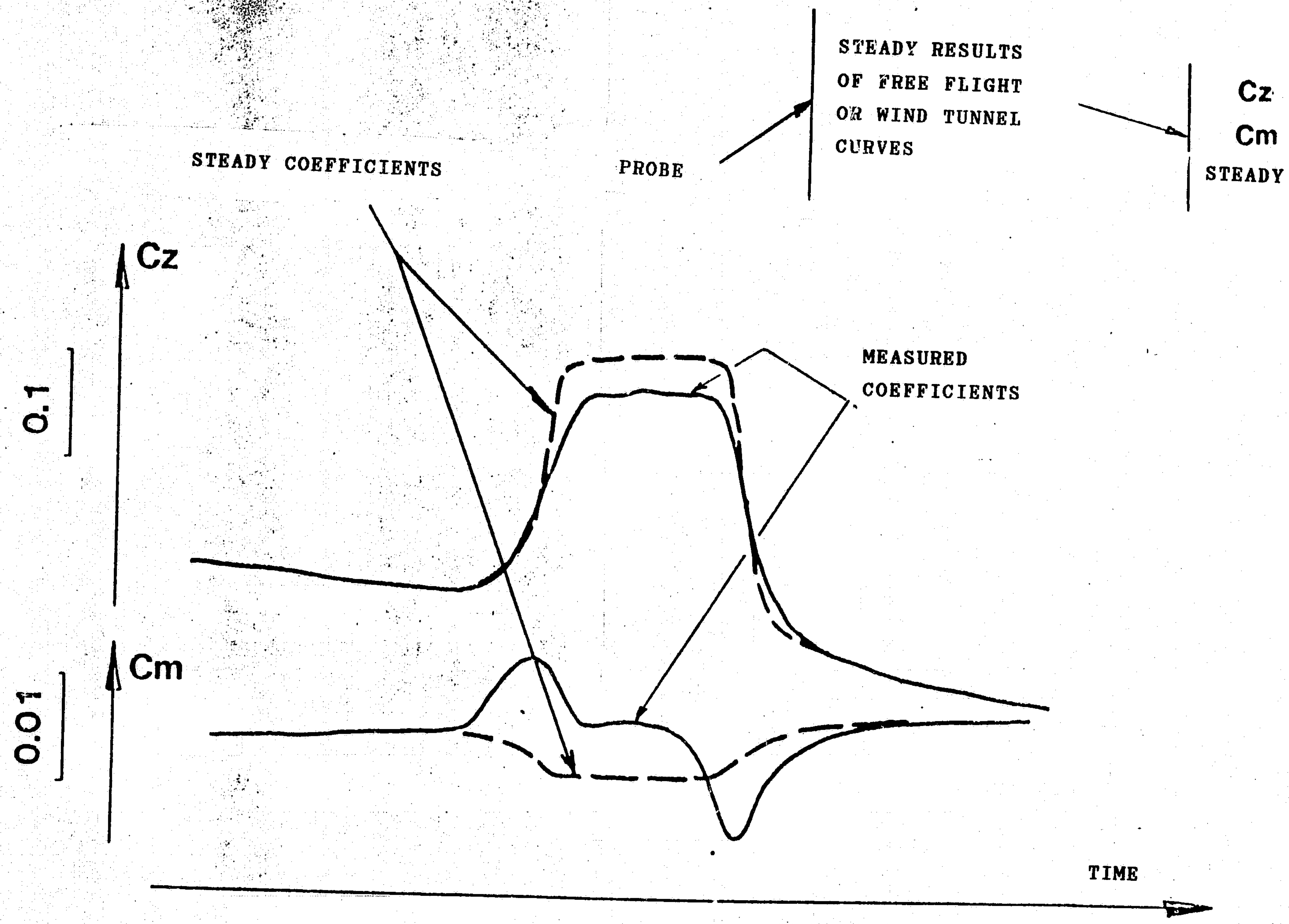

ORIGINAL PAGE IS
OF POOR QUALITY

RESEARCH OF IMPULSE RESPONSES

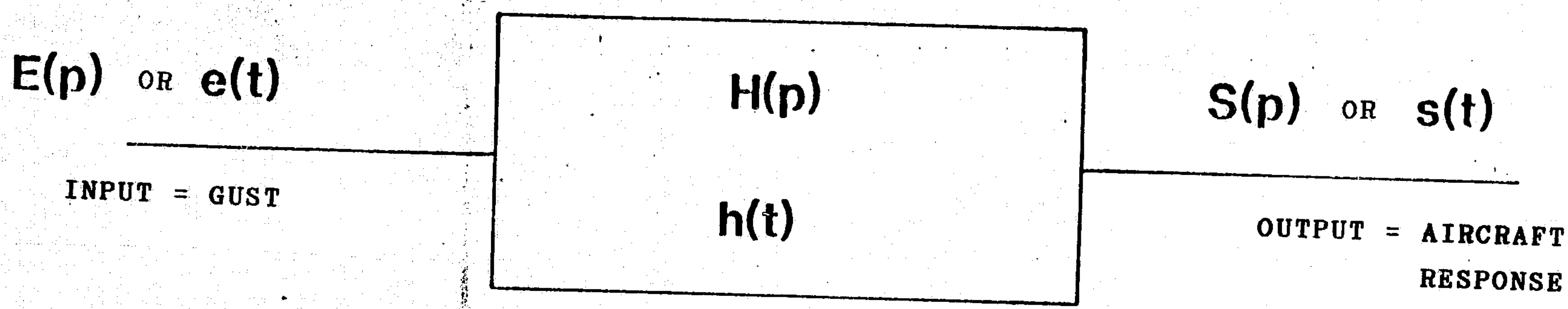

IMPULSE RESPONSE

$$\boxed{Cz_m(t) = Cz_{m_o} + Cz_{m_q} \cdot q(t) + \sum_{i=0}^{p} Cz_{m\alpha_i} \cdot \alpha(t-iT)}$$

OVERALL RESOLUTION $\longrightarrow$ $AX = B$

$A(n, p+3)$

$X(p+3, 2)$

$B(n, 2)$

ORIGINAL PAGE IS
OF POOR QUALITY

Figure 10

Figure 11

FINDING LOCAL COEFFICIENTS

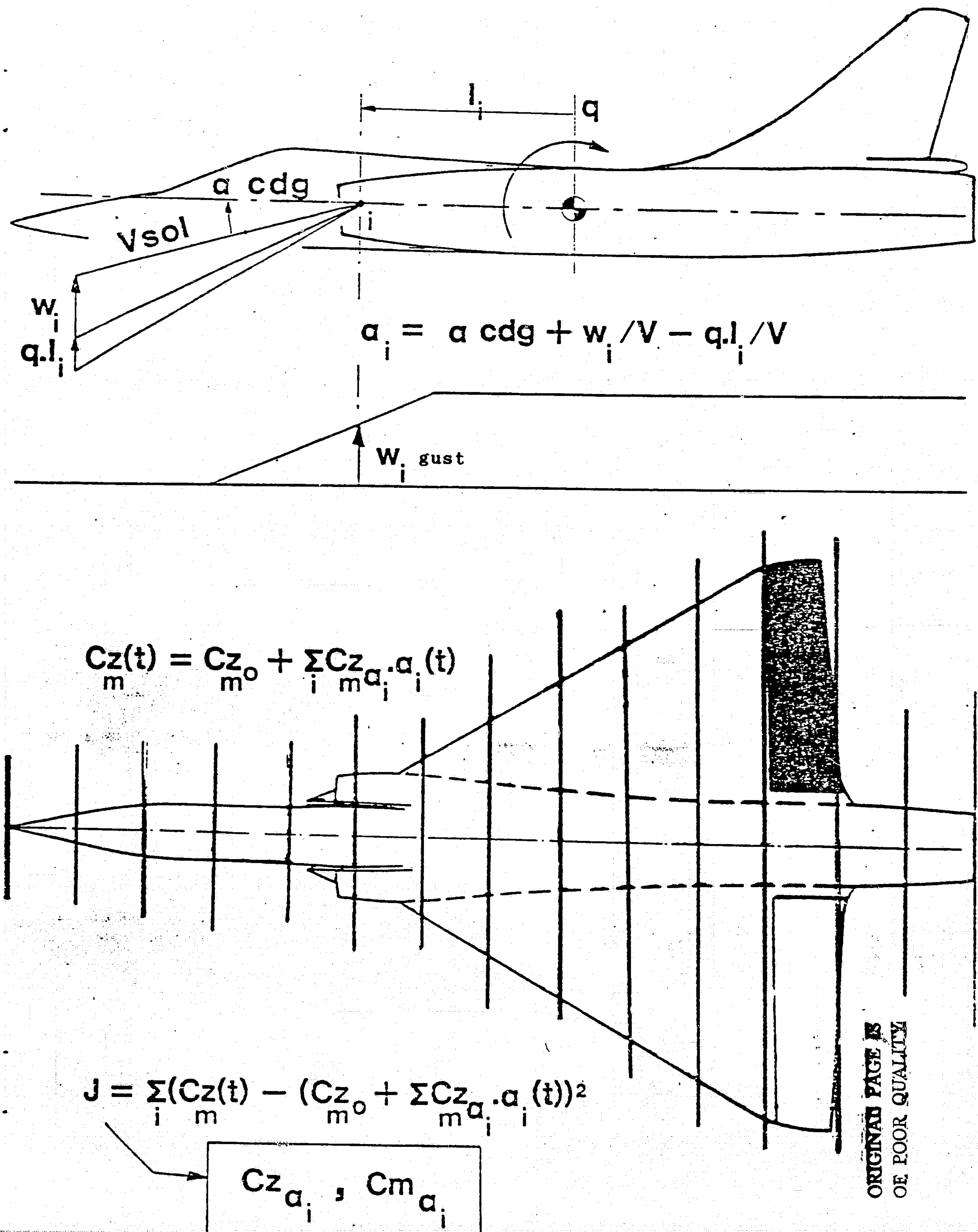

Figure 11

FINDING LOCAL COEFFICIENTS

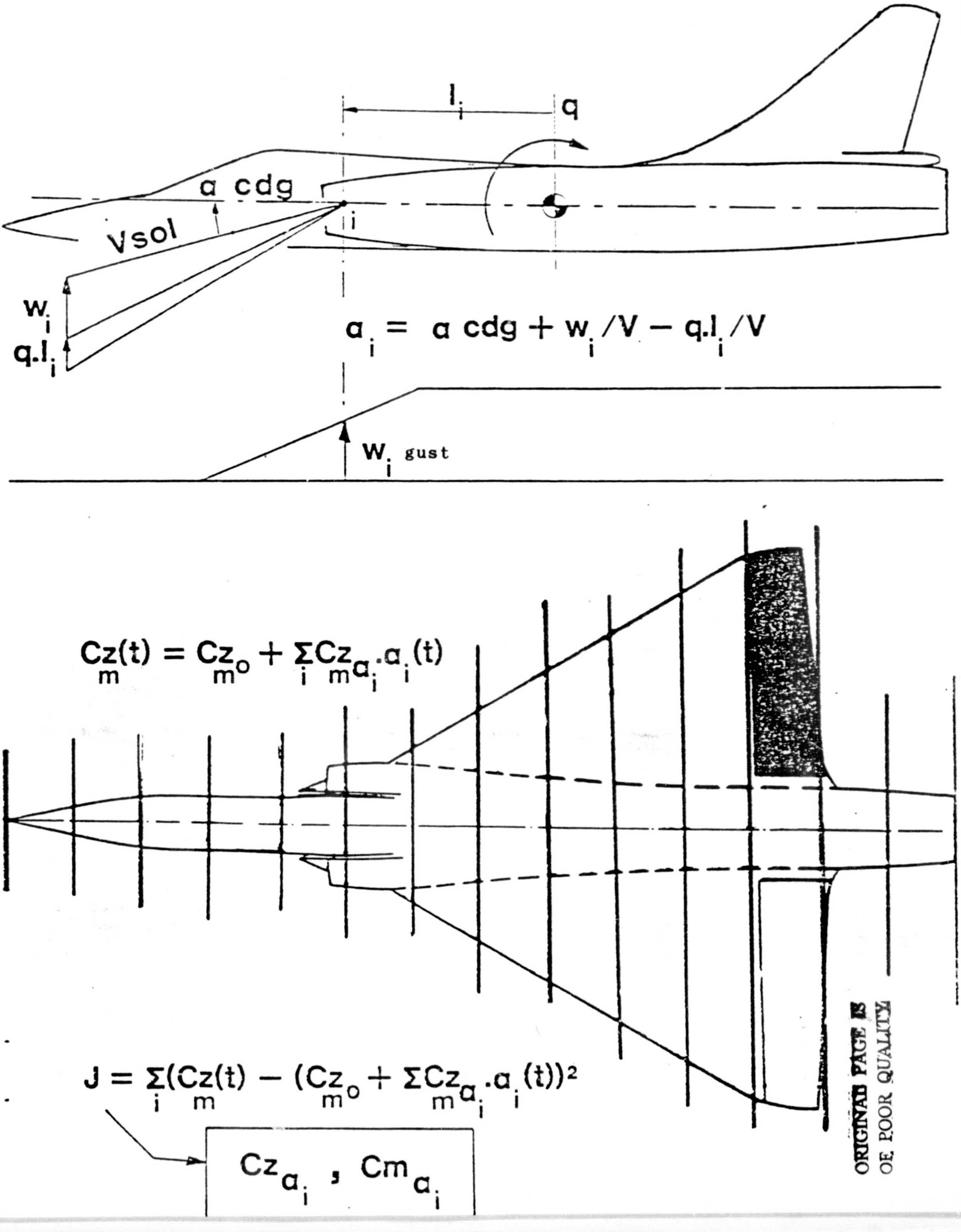

ORIGINAL PAGE IS
OF POOR QUALITY

ANGLE OF INCIDENCE CHOICE

Figure 12

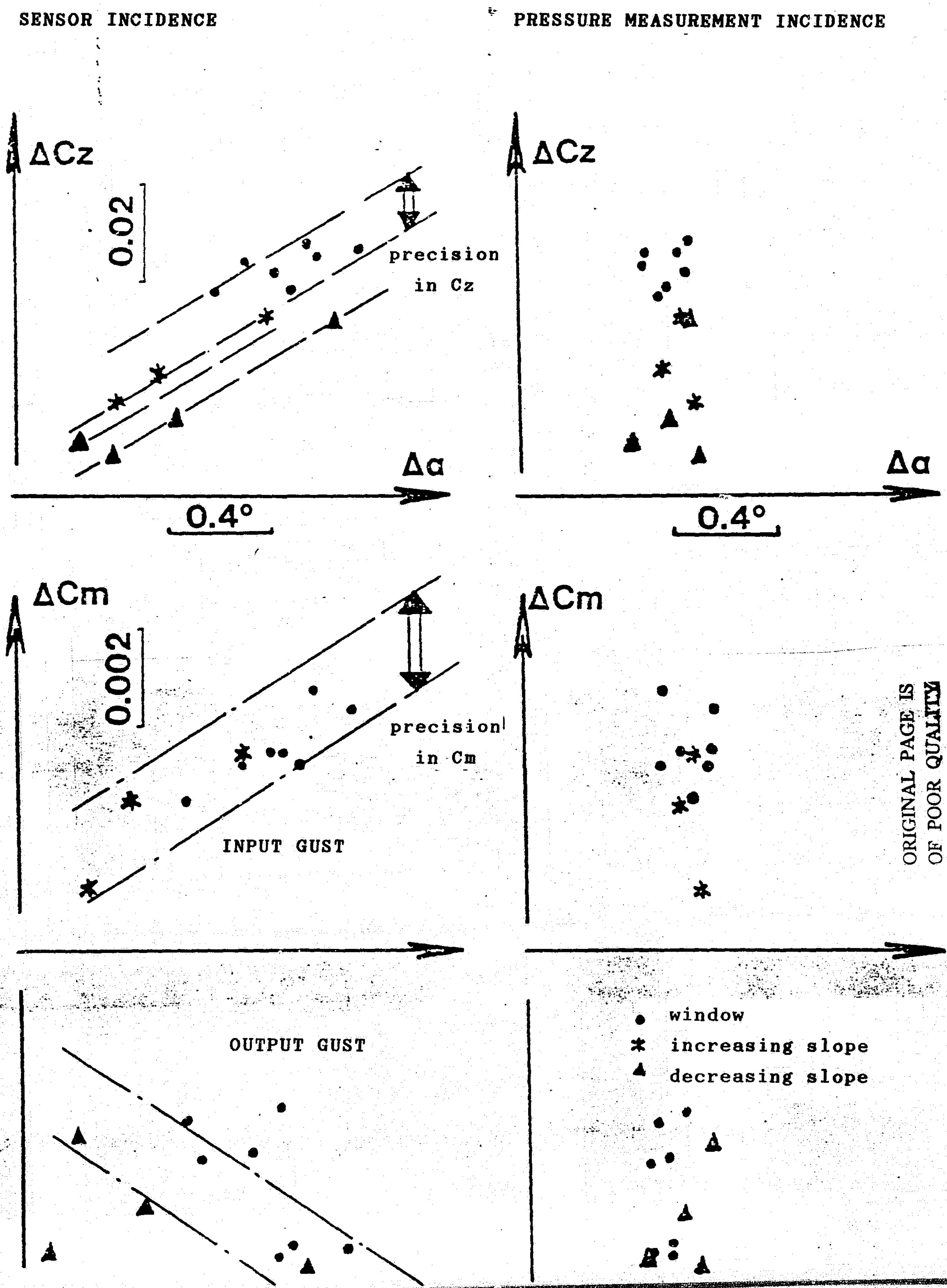

GROSS PROBE SIGNALS

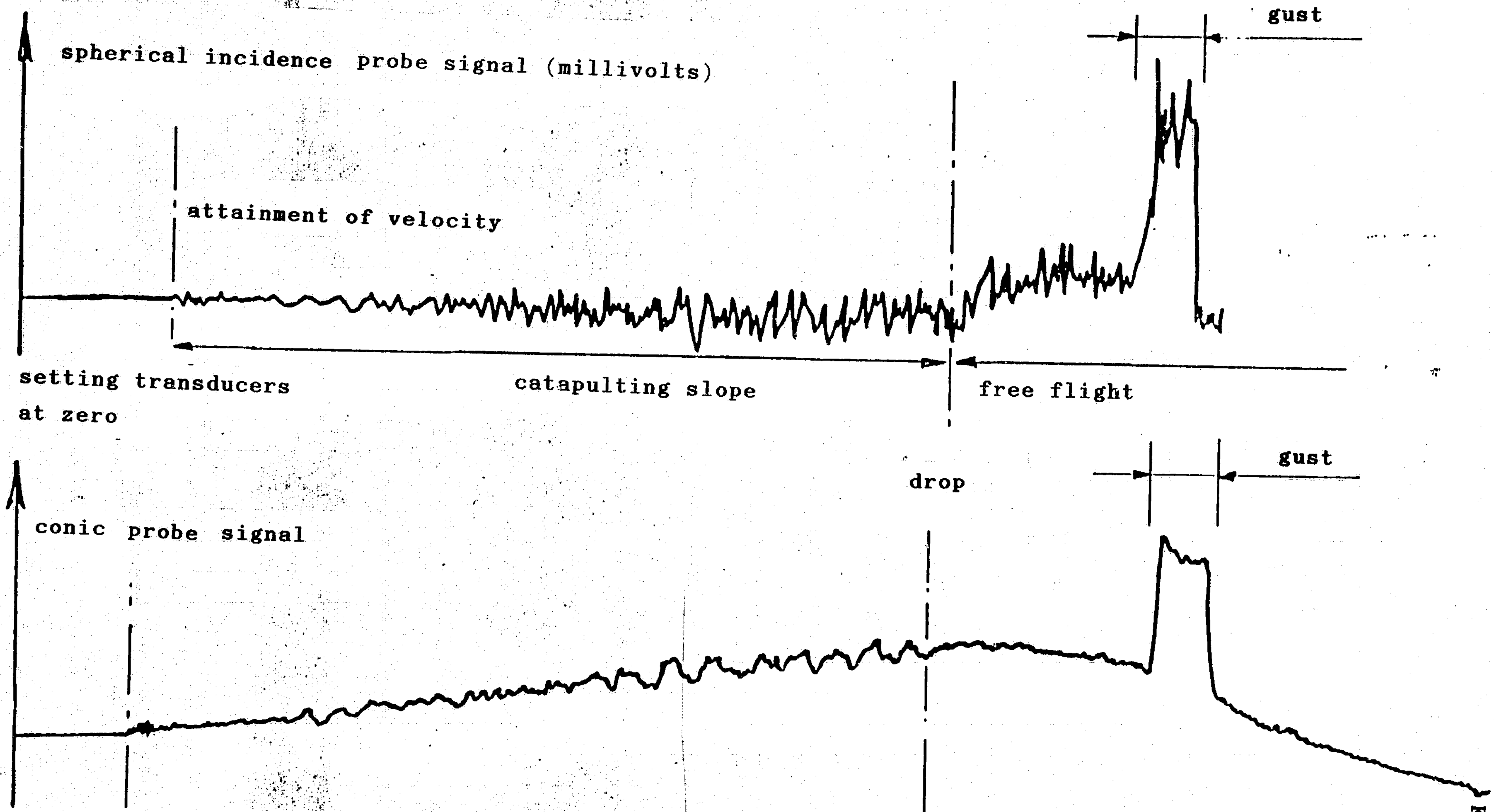

ORIGINAL PAGE IS
OF POOR QUALITY

Figure 13

Figure 14

SENSOR BEHAVIOR OUTSIDE GUST

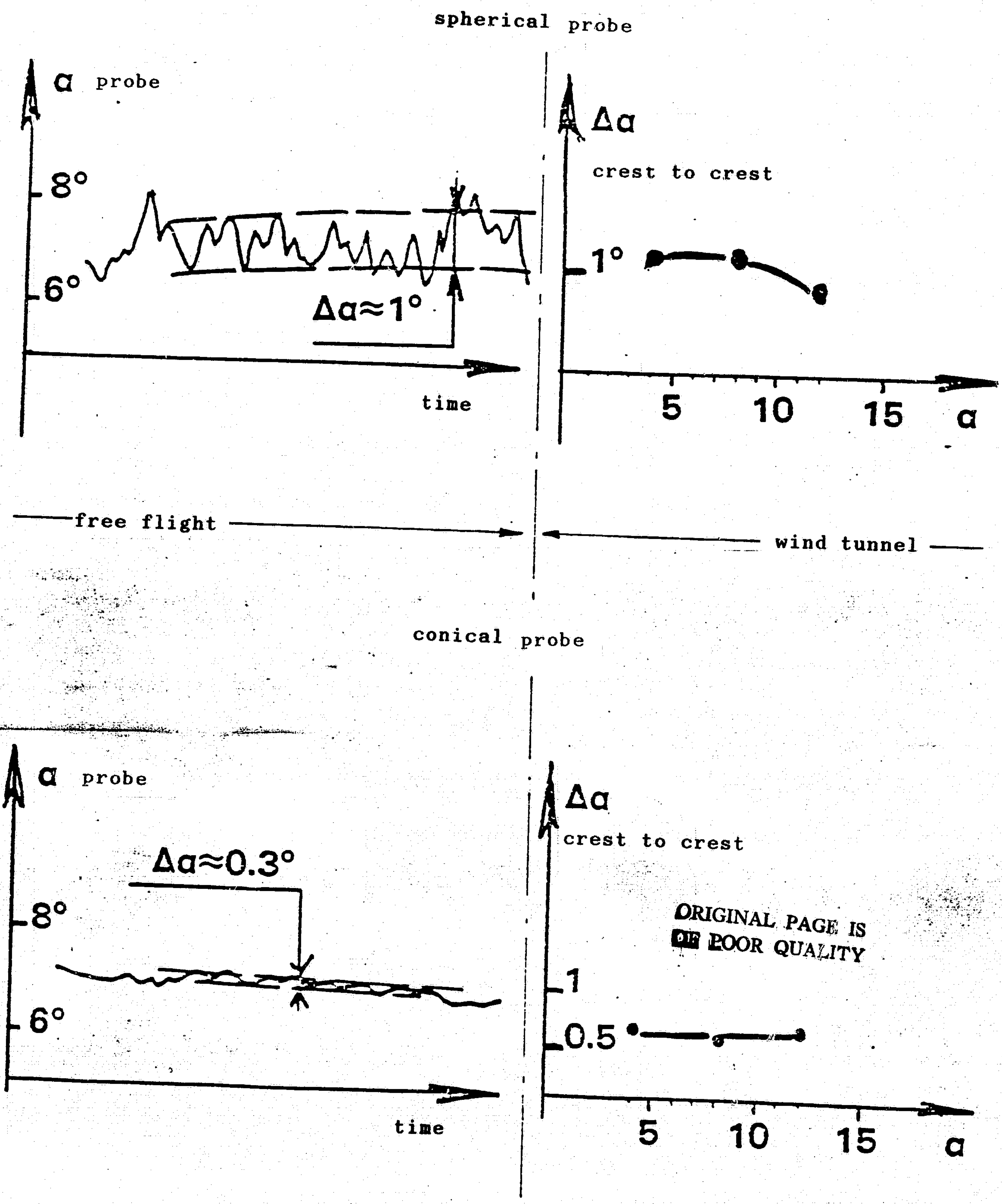

PROBE BEHAVIOR INSIDE GUST

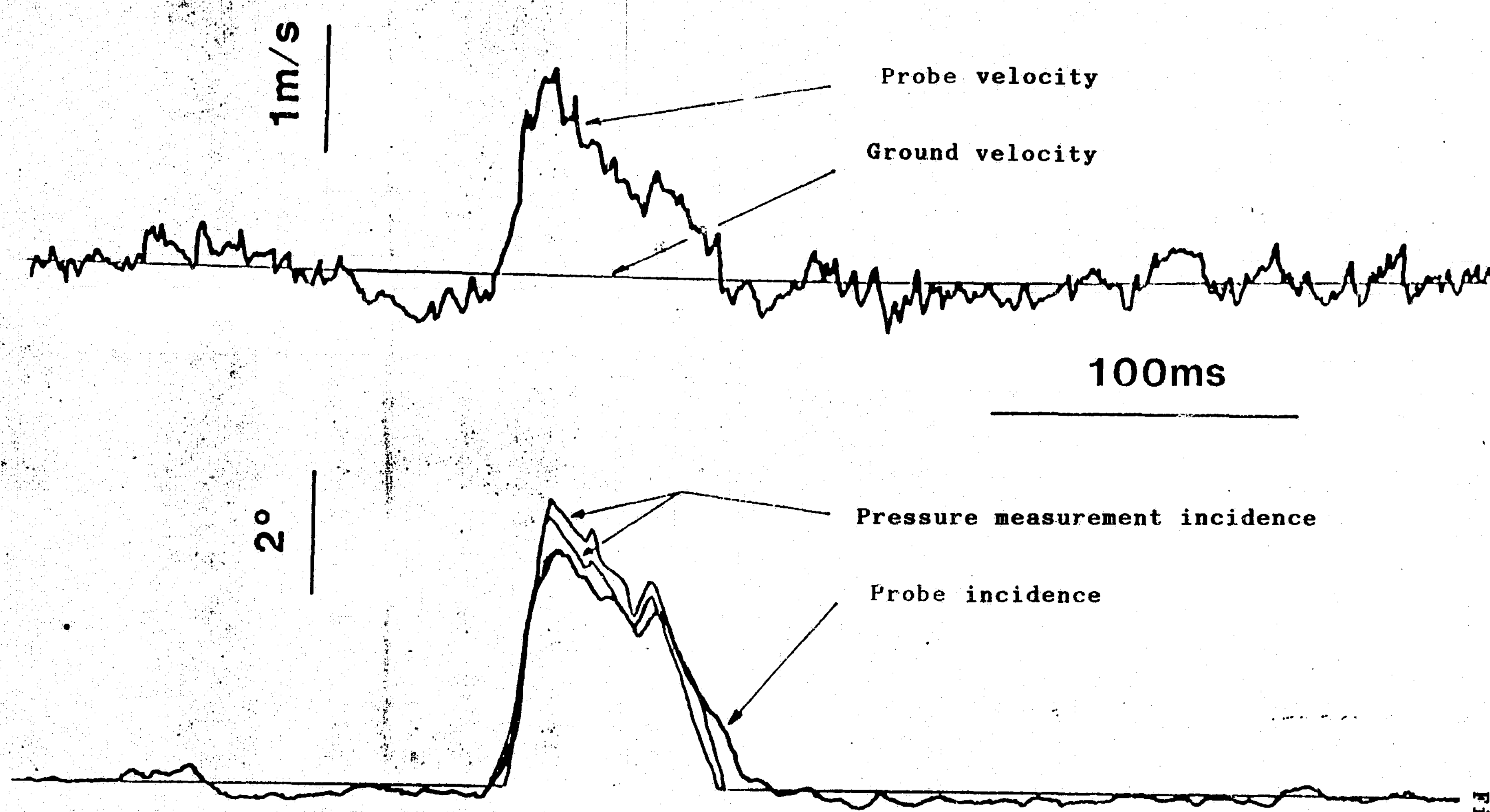

Figure 15

Figure 16

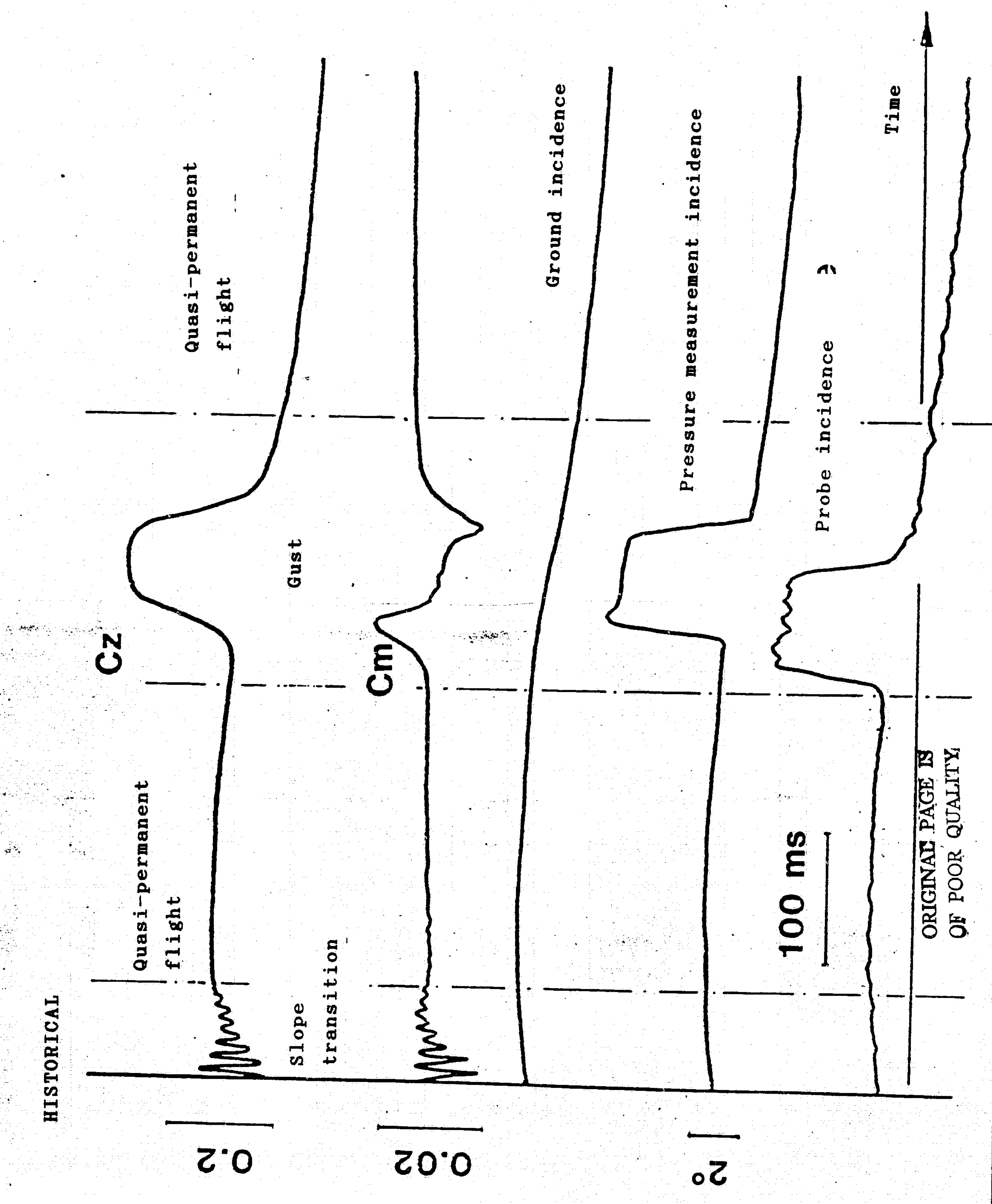
HISTORICAL
Quasi-permanent flight
Slope transition
Quasi-permanent flight
Gust
Cz
Cm
Ground incidence
Pressure measurement incidence
Probe incidence
Time
100 ms
0.2
0.02
2°

Figure 17

COMPARISON FREE FLIGHT WIND TUNNELS

balanced curves

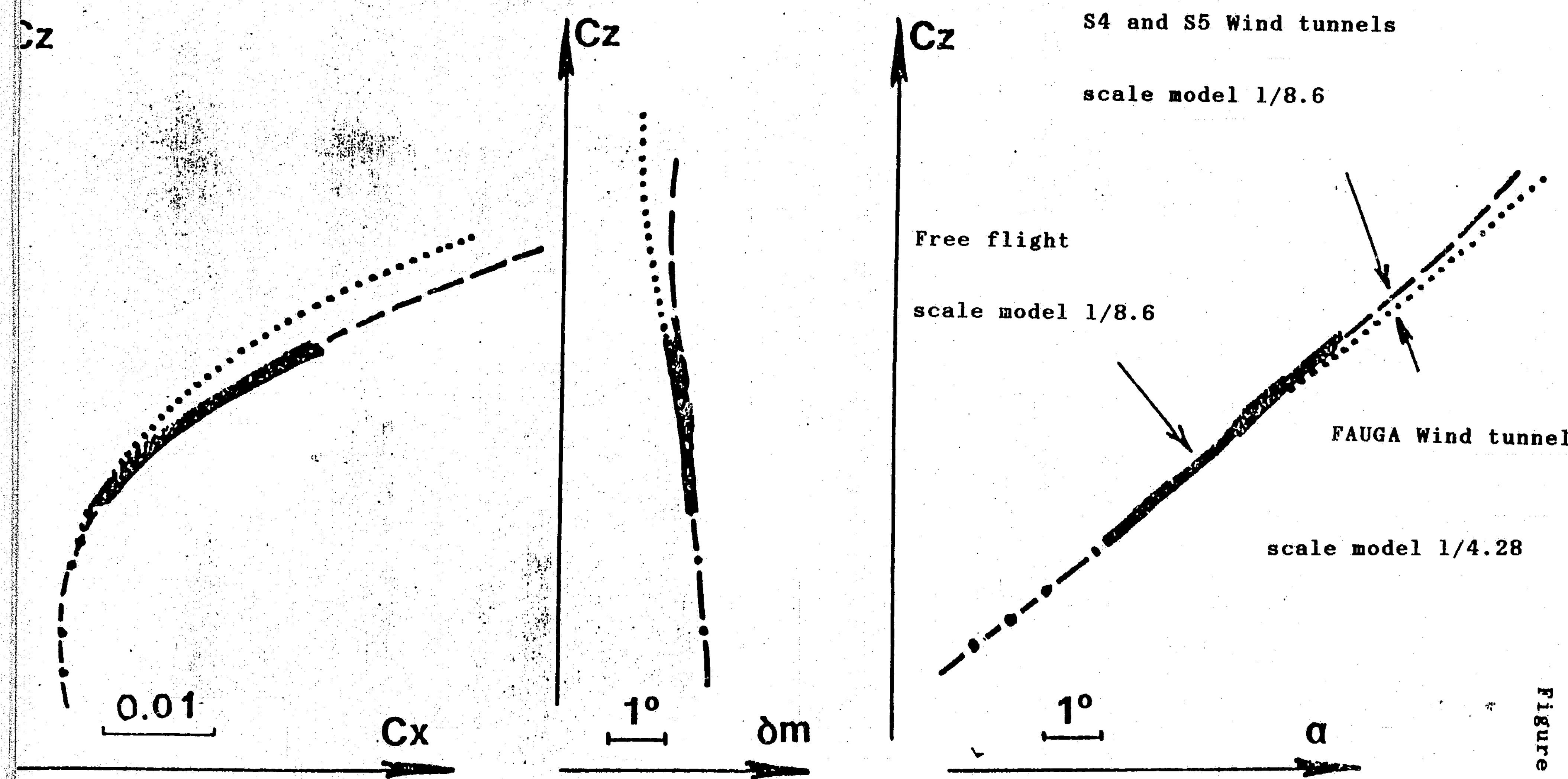

REPEATABILITY 10 FLIGHTS Balanced Coefficients

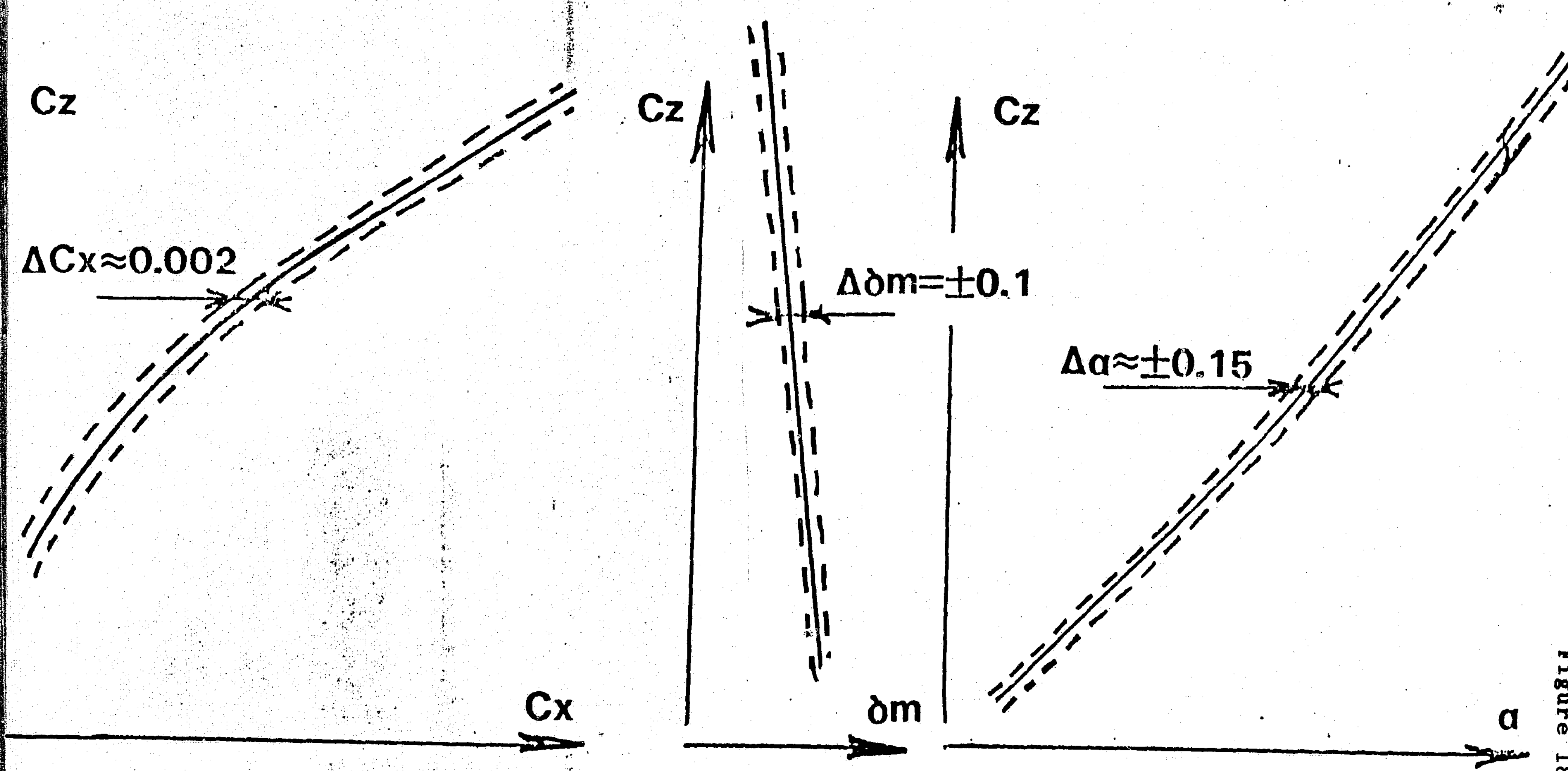

Figure 19

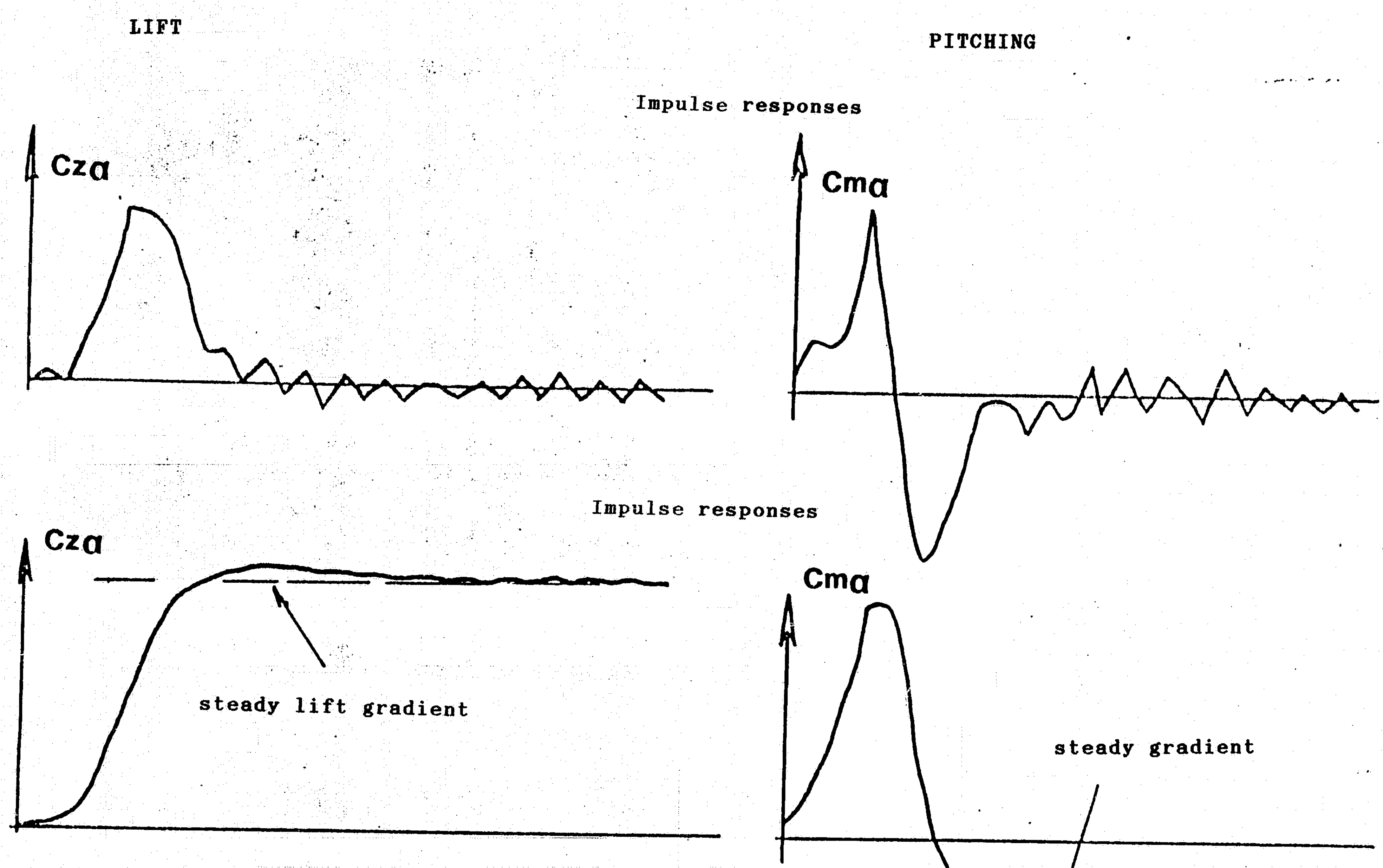
LIFT
PITCHING
Impulse responses
Czα
Cmα
Impulse responses
Czα
steady lift gradient
Cmα
steady gradient

Figure 20

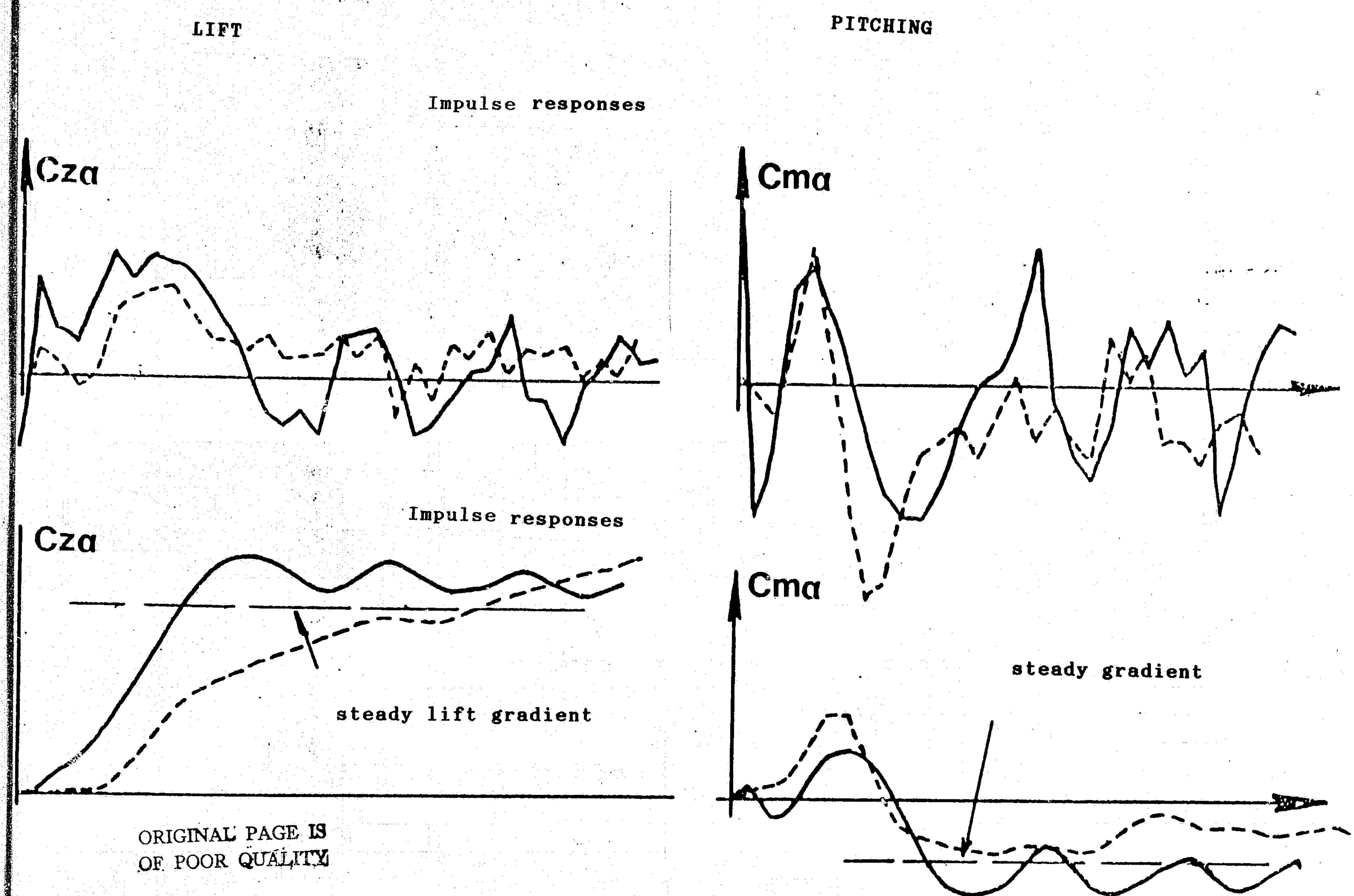
LIFT
PITCHING
Impulse responses
Czα
Cmα
Impulse responses
Czα
Cmα
steady lift gradient
steady gradient

VERTICAL GUST MODELING

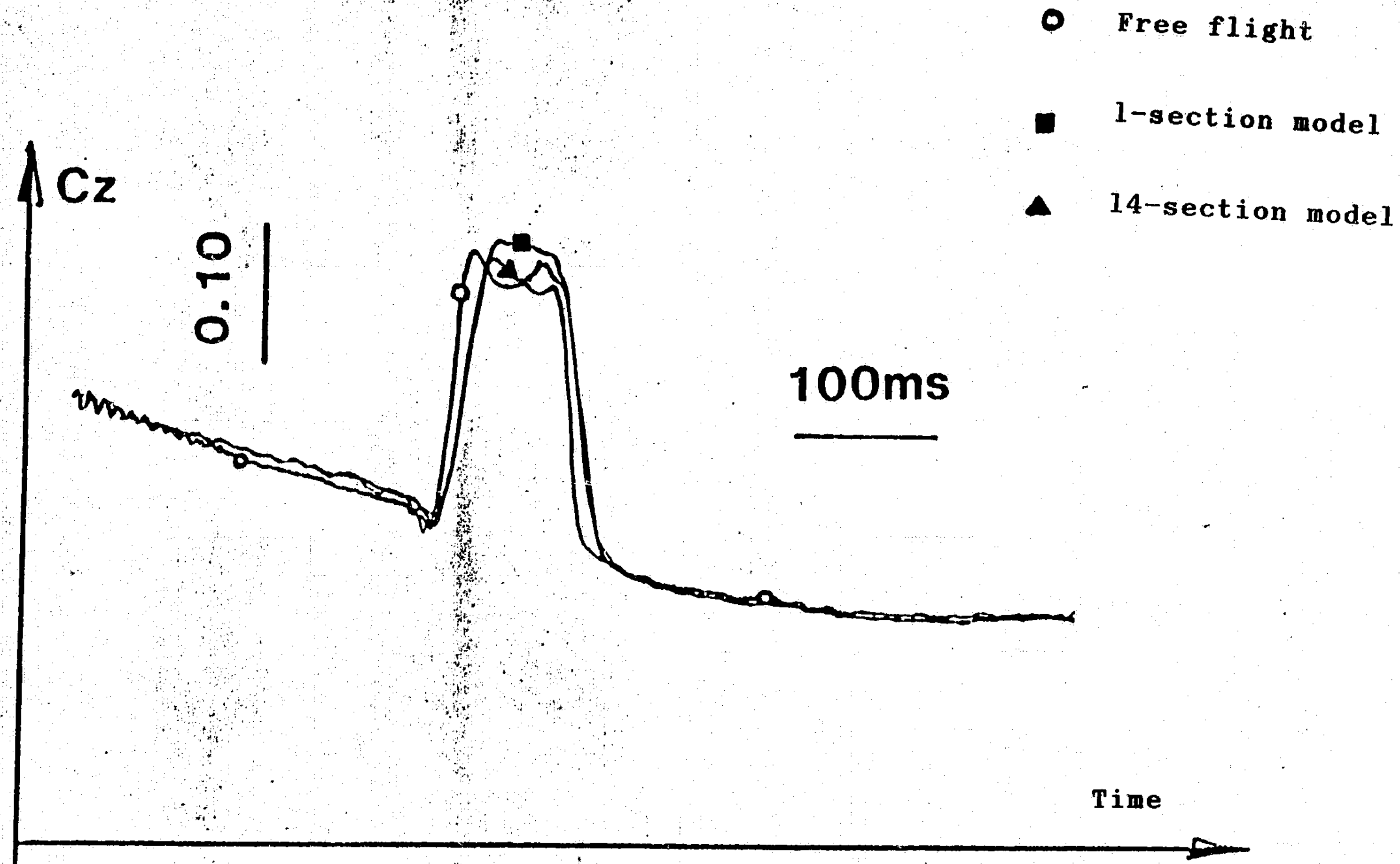

ORIGINAL PAGE IS
OF POOR QUALITY

Figure 21

Figure 22

VERTICAL GUST MODELING